

Augmented Linear Quadratic Tracker for Enhanced Output-Voltage Control of DC-DC Buck Converter

Omer Saleem*, Mohsin Rizwan**, Muaaz Ahmad*

* Department of Electrical Engineering, National University of Computer and Emerging Sciences, Lahore, Pakistan (e-mail: omer.saleem, 1144442@lhr.nu.edu.pk)

** Department of Mechatronics and Control Engineering, University of Engineering and Technology, Lahore, Pakistan (e-mail: mohsin.rizwan@uet.edu.pk)

Abstract: This paper presents a methodic approach to synthesize a robust affine state-feedback controller to enhance the output-voltage tracking control performance of a DC-DC buck converter circuit. The proposed control scheme primarily utilizes a conventional linear-quadratic-tracker (LQT) that renders optimal control decisions based on the state-feedback of output-voltage and inductor-current. Additionally, it employs a feed-forward control term to track the time-varying reference voltage trajectories. Despite its optimality, the LQT lacks robustness in eliminating the steady-state errors and compensating the effects of bounded exogenous disturbances that are caused by high-frequency noises, load-step transients, and modeling errors. In this research, the conventional LQT is equipped with auxiliary tools to dynamically compensate the aforementioned parametric uncertainties. The existing state-space model of the system is augmented with an additional integral-of-error state-variable to eliminate the steady-state fluctuations in output-voltage response. The controller is also retrofitted with a self-tuning capacitor-current control term in order to emulate and deliver the derivative control effort. It rejects the disturbances, compensates the hysteresis effect rendered by the parasitic impedances, and improves the error convergence-rate of the response. The proposed augmented tracking controller is rigorously analyzed via experimental tests to validate its effectiveness.

Keywords: Buck converter, linear quadratic tracker, integral control, capacitor-current, self-tuning control.

1. INTRODUCTION

The buck converter is a static power electronic converter that reduces a direct-current (DC) voltage source from a higher level to a lower level (Olalla et al., 2011). The DC-DC converters are widely used in adjustable motor speed drives, electric vehicles, uninterrupted power supplies, communication equipment, ceiling elevators, computer systems, telephone sets, and inverters, etc (Tahri et al., 2012; Ghosh and Banerjee, 2015). The regulated output-voltage (v_o) response of the buck converter is prone to be degraded by the unprecedented fluctuations in the load impedance or the unregulated DC input voltage (v_{in}). However, this problem is normally solved with the aid of a negative-feedback closed-loop control system in the circuit. Where in, the v_o is continuously compared with the reference voltage (v_{ref}), and the resulting error dynamics are used to adjust the duty-cycle (d) of the active switch in the circuit to stabilize the v_o at the desired reference (Dobra et al., 2007).

A plethora of linear and nonlinear controllers have been proposed in the literature to enhance the output-voltage tracking control and regulation capability of the buck converter (Mariethoz et al., 2010; Lindiya et al., 2012; Pedroso et al., 2013; Hossain et al., 2018). The proportional-integral-derivative controllers are widely used in the industry owing to their simplicity, robustness and model-free nature (Jalilyand et al., 2010; Seshagiri et al., 2016; Mehendran and Ramabdran, 2016). However, finding a trivial set of

controller gains that yield optimal control performance is a cumbersome process (Anbarasi and Muralidharan, 2016). The pole-placement techniques have also been rigorously investigated (Benzaouia et al., 2016). But, as mentioned earlier, appropriate placement of the poles to achieve optimal time-domain control performance is a difficult and time-consuming task (Peretz and Yaakov, 2012). Other model free control techniques that have been proposed in the literature are fuzzy logic controllers (Kumar et al., 2013; Boutouba et al., 2017; Lian et al., 2017). These intelligent controllers require heuristically fabricated logical rule bases. The artificial synthesis of rule-base hinders the fuzzy controllers to optimally cater the nonlinearities associated with the complex systems (Guo et al., 2009). The fractional-order PID controllers introduce additional hyper-parameters to increase the degrees-of-freedom and flexibility of controller design (Bhaumik et al., 2016; Zhu et al., 2014). However, the parameter optimization is a computationally expensive task. Other mentionable control techniques include back-stepping control and sliding mode control (Babazadeh and Maksimovic, 2009; McIntyre et al., 2015; Qi et al., 2018).

The state-space controllers deliver optimal control decisions, since they utilize the full state-feedback of the system along with its linear mathematical model (Lakshmi and Raja, 2014; Akter et al., 2015; Aryani et al., 2017). Extensive research has been done on Linear-Quadratic-Regulators (LQR) as an optimal voltage control scheme for buck converters (Moreira et al., 2011; Dupont et al., 2013; Maccari et al., 2013; Lindiya

et al., 2016). However, despite their optimality, the conventional LQRs severely lack in robustness against dynamic variations in the reference trajectory, load-step changes, line-voltage fluctuations, steady-state errors, and modeling errors (Cui et al., 2014; Saleem and Omer, 2017b). Several augmented versions of the LQR have been proposed in the literature to enhance the reference trajectory tracking performance of the buck converters (Pedroso et al., 2013; Spinu et al., 2014; Tan et al., 2014; Karanjkar et al., 2014; Lee et al., 2016). However, they require extensive computational resources. The conventional LQRs are normally equipped with a feed-forward control term in order to accurately track the time-varying reference trajectories. Such controllers are referred to as the Linear-Quadratic-Trackers (LQTs), (Kiumarsi et al., 2015; Modares et al., 2014; He et al., 2017). The suppression of the modeling-uncertainties and other disturbances still remains a major concern for the LQTs (Ghartemani et al., 2011).

In this research, the robustness of a conventional LQT is enhanced by augmenting it with two additional controlling tools. Firstly, an auxiliary state-variable regarding the integral of error in v_o is introduced in the existing state-space model (Jaen et al., 2006; Ruderman et al., 2008; Naik et al., 2015). The proposed augmentation eliminates the steady-state errors and damps the unnecessary overshoots, undershoots, and oscillations (Reis et al., 2011). Secondly, the existing controller is retrofitted with a control term regarding the derivative of v_o . The derivative controller improves the transitional-times, error-convergence rate, and disturbance-attenuation capability of the system (Corradini et al., 2010; Pitel and Krein, 2009; Lambert et al., 2009). Moreover, it effectively compensates the damping effect rendered by the aforementioned integral control term. However, simultaneously, the derivative operator also inevitably amplifies and injects high frequency noise in the response of v_o . Hence, in this paper, the state-variable regarding the derivative of v_o is replaced with the capacitor-current (i_c) term in the proposed control law (Kapat and Krein, 2012a; Kapat and Krein, 2012b). This augmentation attenuates the effects of hysteresis rendered by the parasitic impedances as well. Once the LQT is equipped with the proposed auxiliary components, the resulting Augmented-Tracking-Controller (ATC) is experimentally tested in real-time and the results are analyzed to justify its efficacy.

2. EXPERIMENTAL SETUP

The buck convertor is a DC-DC power electronic converter that reduces and regulates a given DC input voltage source to a desired level. The circuit diagram of the buck converter is shown in Fig. 1. The high-frequency switching transistor in the converter's circuit chops down the DC input voltage into a rectangular waveform. This rectangular waveform is fed to a low-pass filter formed by the inductor-capacitor network which only allows the DC component (average value) of the waveform to pass through.

The output voltage of convertor, given by (1), can be regulated by varying the duty-cycle ratio (d) of the transistor. The duty-cycle ratio is given by (2).

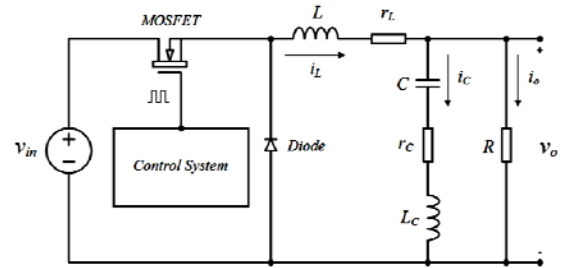


Fig. 1. Buck converter circuit.

$$v_o = d \times v_{in} \quad (1)$$

$$d = \frac{t_{on}}{t_{on} + t_{off}} \quad (2)$$

where, t_{on} and t_{off} is denoted as the on-time and off-time of switching period, respectively. In case of any fluctuations in the load-resistance (R) or v_{in} , the negative-feedback controller changes the duty-cycle of the switching period in order to maintain the v_o at the reference value. During the on-time of switch, the entire current from the input passes through the capacitor and the load-resistor, while charging the inductor in its path. The diode stays reverse biased during the on-time. During the off-time of switch, the input current supply to the remaining circuit is cut-off. However, the diode is forward-biased which closes the circuit loop and allows the inductor to discharge through the capacitor and load-resistor (Mohan et al., 2007). The hardware setup and the mathematical model of the system are presented in the following sub-sections.

2.1 Hardware setup

The output-voltage (v_o) is measured with the aid of a voltage sensor. The inductor-current (i_L) is measured via a shunt resistor of 0.01Ω , 5.0W. These sensors are present on-board the buck converter module, shown in Fig. 2. The real-time analog measurements of the aforementioned electrical states are fed to a 32-bit embedded microcontroller (Antão et al., 2014). The microcontroller filters and digitizes the acquired sensor-data at a sampling frequency of 1000 Hz.

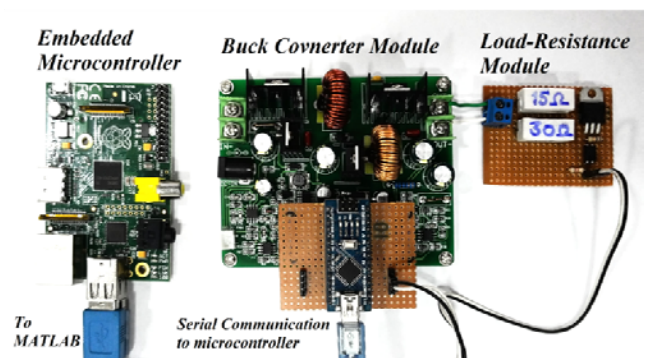


Fig. 2. Hardware setup.

The microcontroller serially transmits the conditioned sensor-data, at 9600 bps, to a MATLAB based computer application (Duong et al., 2017; Bagewadi and Damhare, 2017). The computer application is used for the graphical visualization of the state-variations in real-time. The embedded control system generates optimal correctional commands based on the variations in state-feedback. These commands are

transformed into high-frequency Pulse-Width-Modulated (PWM) signals. The PWM commands drive the MOSFET (Metal-Oxide-Surface-Field-Effect-Transistor) switch in the convertor's circuit via a dedicated optically isolated PWM amplifier. In this research, the switching frequency of the MOSFET is 100 kHz. The load-resistance (R) is formed by the parallel combination of two fixed resistors; 15.0 Ω and 30.0 Ω . An NPN Power Transistor (M) is connected in series with the 30.0 Ω resistor, only. Under normal conditions, the transistor M is kept turned-on. Consequently, the overall R of the circuit is equal to 10.0 Ω . However, when the transistor M is turned-off, the 30.0 Ω resistor gets excluded from the remaining circuit. This phenomenon introduces a 50% step-increment in the overall R , making it 15.0 Ω .

2.2 Mathematical model

The state-space model of a linear dynamical system is given by (3) and (4).

$$\dot{x}(t) = \mathbf{A}x(t) + \mathbf{B}u(t) \quad (3)$$

$$y(t) = \mathbf{H}x(t) + \mathbf{F}u(t) \quad (4)$$

where, $x(t)$ is the state-vector, $y(t)$ is the output-vector, $u(t)$ is the control signal, \mathbf{A} is the state matrix, \mathbf{B} is the input matrix, \mathbf{H} is the output matrix, and \mathbf{F} is the feed-forward matrix. The state-vector and the control input of the buck converter are defined in (5).

$$x(t) = [v_o(t) \quad i_L(t)]^T, \quad u(t) = d(t) \quad (5)$$

where, $d(t)$ is the time-varying duty-cycle signal. The averaged mathematical model of the converter is experimentally identified. The matrices \mathbf{A} , \mathbf{B} , \mathbf{H} , and \mathbf{F} of the buck converter's state-space model are defined in (6), (Kapat and Krein, 2012b; Priewasser et al., 2014).

$$\mathbf{A} = \begin{bmatrix} -\frac{1}{C(R+r_c)} & \frac{R}{C(R+r_c)} \\ \frac{R}{L(R+r_c)} & -\frac{(r_L+r_c||R)}{L} \end{bmatrix}, \quad \mathbf{B} = \begin{bmatrix} 0 \\ \frac{v_{in}}{L} \end{bmatrix}, \quad \mathbf{H} = [1 \quad 0], \quad \mathbf{F} = 0 \quad (6)$$

The design parameters of the buck converter circuit, used in this research, are identified in Table 1.

3. LINEAR QUADRATIC TRACKER

The linear quadratic tracker (LQT) is a model-based tracking control mechanism that uses the affine state-feedback to deliver optimal control effort.

Table 1. Design parameters of buck-converter circuit.

Parameters	Symbol	Values
Load-resistance	R	10 Ω
Inductance	L	330 μH
Capacitance	C	1000 μF
ESR of capacitor	r_c	0.08 Ω
ESR of inductor	r_L	0.07 Ω
Input voltage	v_{in}	30 V
Maximum output power	P_{out}	100 W

*ESR = Equivalent Series Resistance

The LQT consists of the usual state-feedback of the linear dynamical system along with additional feed-forward control term. The feed-forward control term depends on the reference signal vector, $r(t)$. The vector $r(t)$ is expressed in (7).

$$r(t) = [v_{ref}(t) \quad 0]^T \quad (7)$$

where, $v_{ref}(t)$ is the time-varying reference voltage signal. The LQT scheme minimizes the quadratic performance index, given by (8), in order to generate optimal control decisions (Lewis et al., 2012).

$$J = \frac{1}{2} \int_0^T [(x(t) - r(t))^T \mathbf{Q}(x(t) - r(t)) + d(t)^T \mathbf{R}d(t)] dt \quad (8)$$

where, \mathbf{Q} and \mathbf{R} are the intermediate-state and control weighting matrices, respectively. They are chosen such that; $\mathbf{Q} = \mathbf{Q}^T \geq 0$ and $\mathbf{R} = \mathbf{R}^T > 0$. Owing to the quadratic nature of the cost function, the control signal is proportional to the square of variations in the states. Thus, if the state-variations are large; the minimization and, hence, the convergence-rate is faster. The weighting matrices used in this research are heuristically selected and are given by (9).

$$\mathbf{Q} = \begin{bmatrix} 1 & 0 \\ 0 & 1 \end{bmatrix}, \quad \mathbf{R} = 10 \quad (9)$$

The optimal affine control decisions are evaluated via the mathematical expression shown in (10), (Ruderman et al., 2008; Lewis et al., 2012).

$$d(t) = -\mathbf{K}x(t) + K_{ff}v_{ref}(t) \quad (10)$$

$$\text{where, } \mathbf{K} = \mathbf{R}^{-1}\mathbf{B}^T\mathbf{P} \quad (11)$$

$$\text{and, } K_{ff} = -\mathbf{R}^{-1}\mathbf{B}^T((\mathbf{A} - \mathbf{B}\mathbf{K})^T)^{-1}\mathbf{H}^T\mathbf{Q} \quad (12)$$

The gain vector, \mathbf{K} , helps to relocate the poles of the system in order to synthesize an optimal controller. The optimal gain vector depends on a symmetric positive definite matrix, \mathbf{P} , as shown in (11). The matrix, \mathbf{P} , for the given system is evaluated by solving the Algebraic Riccati Equation, shown in (13).

$$\mathbf{A}^T\mathbf{P} + \mathbf{P}\mathbf{A} - \mathbf{P}\mathbf{B}\mathbf{R}^{-1}\mathbf{B}^T\mathbf{P} + \mathbf{H}^T\mathbf{Q}\mathbf{H} = 0 \quad (13)$$

In order to optimize the trajectory tracking response, a feed-forward (ff) control term is constituted in the LQT control law as well. This term compensates the dynamic changes in the reference trajectory. The feed-forward gain (K_{ff}), shown in (12), depends on the output of the adjoint of the closed-loop plant when driven by $v_{ref}(t)$, (Lewis et al., 2012). Based on the system-description provided in the previous section, the evaluated state-feedback gain vector (\mathbf{K}) and the feed-forward gain (K_{ff}) are given by (14) and (15), respectively.

$$\mathbf{K} = [K_{v_o} \quad K_{i_L}] = [0.2403 \quad 0.1102] \quad (14)$$

$$K_{ff} = -0.306 \quad (15)$$

4. PROPOSED CONTROL SCHEME

This section presents the synthesis of the proposed state-feedback control scheme. The conventional LQT is at the heart of the proposed controller. However, it is equipped with two additional controlling mechanisms in order to improve its robustness in the time-domain. Firstly, the existing state-space model of the motor is modified by retrofitting it with

an auxiliary state-variable regarding the integral of error. Secondly, the control system is augmented with an active disturbance-rejection-controller. The mathematical derivation of the proposed control scheme is as follows.

4.1 Auxiliary integral state-variable

In order to improve the steady-state performance of the control scheme, the existing LQT architecture is retrofitted with an auxiliary control term that delivers the correctional efforts based on the integral of error in v_o . The augmentation of integral controller effectively eliminates the steady-state errors, inhibits the overshoots (or undershoots), and damp the oscillations. The time-integral of error is given by (16).

$$\varepsilon(t) = \int_0^t e(\tau) d\tau \quad (16)$$

$$\text{such that, } e(t) = v_{ref}(t) - v_o(t) \quad (17)$$

With the introduction of the integral-of-error (ε) as an additional state-variable in the existing state-space model, the augmented controller is denoted as the Linear-Quadratic-Integral-Tracker (LQIT). The augmented state-vector is given by (18).

$$\hat{x}(t) = [v_o(t) \quad i_L(t) \quad \varepsilon(t)]^T \quad (18)$$

The revised state-space model is given by (19).

$$\begin{bmatrix} \dot{v}_o \\ \dot{i}_L \\ \dot{\varepsilon} \end{bmatrix} = \begin{bmatrix} -\frac{1}{C(R+r_c)} & \frac{R}{C(R+r_c)} & 0 \\ R & -(r_L+r_c||R) & 0 \\ -\frac{1}{L(R+r_c)} & \frac{1}{L} & 0 \end{bmatrix} \begin{bmatrix} v_o \\ i_L \\ \varepsilon \end{bmatrix} + \begin{bmatrix} 0 \\ v_{in} \\ L \\ 0 \end{bmatrix} d + \begin{bmatrix} 0 \\ 0 \\ 1 \end{bmatrix} v_{ref} \quad (19)$$

The output vector, H , is also modified according to (20).

$$H = [1 \quad 0 \quad 0] \quad (20)$$

The Q matrix is augmented with a small weight for the ε . The updated weighting matrices and $r(t)$ vector are given by (21).

$$\hat{Q} = \begin{bmatrix} 1 & 0 & 0 \\ 0 & 1 & 0 \\ 0 & 0 & 0.001 \end{bmatrix}, \quad \hat{R} = 10, \quad \hat{r}(t) = [v_{ref}(t) \quad 0 \quad 0]^T \quad (21)$$

Consequently, the LQIT control law is given by (22).

$$d(t) = -\hat{K}\hat{x}(t) + \hat{K}_{ff}v_{ref}(t) \quad (22)$$

The augmented gain vector, \hat{K} and \hat{K}_{ff} , are given by (23) and (24), respectively.

$$\hat{K} = [\hat{K}_{v_o} \quad \hat{K}_{i_L} \quad \hat{K}_{\varepsilon}] = [0.2407 \quad 0.1108 \quad -0.014] \quad (23)$$

$$\hat{K}_{ff} = 0 \quad (24)$$

The feed-forward gain of the LQIT is zero. It is justified because the expression of $\varepsilon(t)$ includes the dynamic variations of v_{ref} as well, apart from eliminating the steady-state fluctuations.

4.2 Disturbance rejection controller

The LQIT is equipped with a Disturbance-Rejection-Controller (DRC) as well. It attenuates the bounded exogenous disturbances that are caused by the modeling uncertainties, load-step transients, and fluctuations in v_{in} . A control term acting directly on the time-derivative of v_o is needed. Apart from enhancing the controller's robustness against the aforementioned disturbances, the derivative of v_o also enhances its phase margin and global asymptotic convergence. This feature is particularly useful in tracking the time-varying trajectories (Saleem et al., 2017), and compensating the damping effects introduced by the auxiliary integral control term. However, the derivative action has some demerits. The derivative-operator inevitably amplifies and injects high frequency noise in the closed-loop system. The parasitic impedances in the circuit also impede the derivative-controller's performance. These impedances majorly include the Equivalent-Series-Resistance (ESR) and Equivalent-Series-Inductance (ESL) of the capacitor (C). This phenomenon leads to large overshoots (or undershoots) during large-signal transients and abrupt bipolar fluctuations during small-signal transients (Kapat and Krein, 2012b). The calculation of the derivative term via the extended-state-observers or tracking-differentiators is a cumbersome and computationally expensive process.

A tangible solution is to directly measure and control the capacitor-current, instead of computing the derivative of v_o in every sampling interval (Kapat and Krein, 2012a). The practical model of the output capacitor, C , is given by (25).

$$\frac{dv_o(t)}{dt} = L_c \frac{d^2 i_c(t)}{dt^2} + r_c \frac{di_c(t)}{dt} + \frac{i_c(t)}{C} \quad (25)$$

where, L_c is the ESL of the capacitor, as shown in Fig. 1. Its value is 0.1 μ H. With the inclusion of random disturbances in the capacitor model, the capacitor-current (i_c) of the buck convertor can be expressed according to (26).

$$i_c(t) \approx \frac{r_c}{r_c C - L_c} \left(e^{\frac{-t}{r_c C}} - e^{\frac{-r_c t}{L_c}} \right) C \left(\frac{dv_o(t)}{dt} \right) \quad (26)$$

If the value of parasitics (ESR and ESL) is negligibly small, then i_c becomes equal to $C \left(\frac{dv_o}{dt} \right)$. Therefore, instead of computing the derivative of v_o , the proposed control scheme directly uses the i_c . The instantaneous variations in i_c are measured with the aid of a shunt power resistor of 0.01 Ω (less than the value of capacitor's ESR). The utilization of the i_c improves the time-optimality of the control effort (Kapat and Krein, 2012a). It compensates the effects of hysteresis caused by the parasitic impedances. It renders insignificant effect on the closed-loop bandwidth and stability. It reinforces the feed-forward controller with information regarding the real-time variations in the load-current and i_L . It enhances the system's disturbance-rejection capability and offers minimum-time load-transient recovery (Pitel and Krein, 2009; Lambert et al., 2009). The DRC used in this research is given by (27).

$$d_{arc}(t) = -K_d i_c(t) \quad (27)$$

where, K_d is the derivative-gain. A fixed value of K_d in the DRC may not be very beneficial. Although it improves the transient response of the system, but, it also inevitably injects persistent fluctuations in the steady-state response. This phenomenon impedes the control action yielded by the auxiliary integral controller. Hence, the value of K_d is adaptively modulated by a nonlinear function of error. Several nonlinear functions are proposed in literature for the adaptive self-tuning of the controller gains (Seraji, 1998; Guo et al., 2012; Saleem and Omer, 2017a). The proposed technique requires a smooth, symmetrical, and differentiable function. Therefore, a Hyperbolic-Secant-Function depending on the error signal, $e(t)$, is used (Isayed and Hawwa, 2007). The error-dependent K_d function is given by (28).

$$K_d(e) = 0.05 + 1.84(1 - \text{sech}(\alpha \times e(t))) \quad (28)$$

where, α is the variance of the function. In this research, its value is heuristically selected to be 2.71 via trial-and-error method. The waveform of the K_d function is shown in Fig. 3. The waveform clearly manifests that, owing to the large value of K_d , the DRC contributes significant correctional effort when the error is large (during transients).

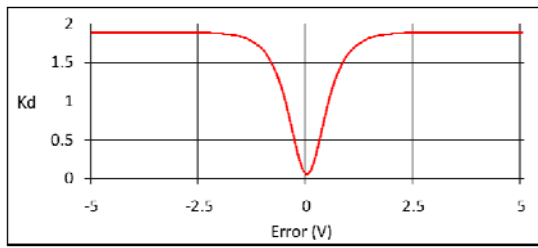


Fig. 3. Waveform of derivative-gain function.

The magnitude of K_d gradually decreases as the error reduces, or as the response converges towards the reference. The K_d becomes negligible when the error is small, or as the system settles in the steady-state.

4.3 Augmented tracking controller

With the addition of the aforementioned individual control mechanisms in the existing LQT architecture, the resulting Augmented-Tracking-Controller (ATC) is given by (29).

$$d(t) = -\hat{K}\hat{x}(t) + \hat{K}_{ff}v_{ref}(t) + d_{arc}(t) \quad (29)$$

A simplified version of control law in (29) is given by (30).

$$d(t) = -[\hat{K}_{v_o} \quad \hat{K}_{i_L} \quad \hat{K}_{\epsilon}] \begin{bmatrix} v_o \\ i_L \\ \epsilon \end{bmatrix} - K_d(e)i_c(t) \quad (30)$$

The structure of ATC is shown in Fig. 4. The ATC algorithm is robust, simple, and computationally efficient with respect to its practical implementation. Due to the introduction of auxiliary integral state-variable in the control system, the \hat{K}_{ff} reduces to zero. The remaining control law simply becomes a fixed-gain LQI controller (Ruderman et al., 2008). The evaluation of the constant gain vector, \hat{K} , does not put any recursive computational burden on the embedded controller in real-time. The self-tuning DRC term improves the time-optimality of the response using a simple pre-defined

nonlinear scaling function of error. Hence, it does not add to the computational complexity of the control system either.

5. TESTS AND RESULTS

The voltage control performances of the LQT, LQIT, and ATC are comparatively analyzed via the following ‘hardware-in-the-loop’ experimental tests. In all the test-cases, a +30.0 V DC signal is supplied as v_{in} to the buck converter from a variable lab-bench power supply.

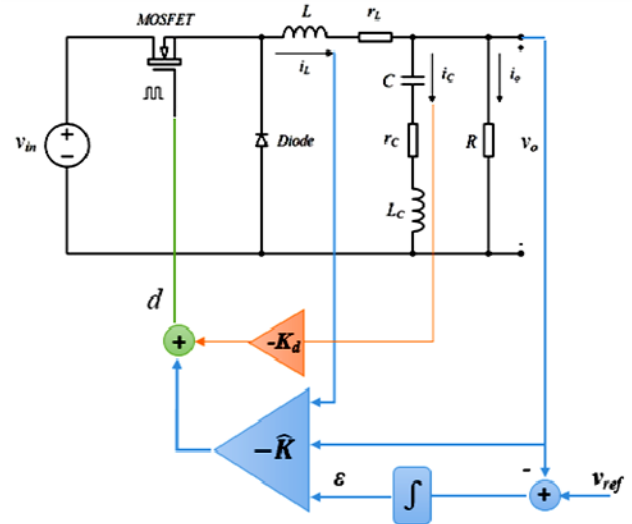


Fig. 4. Augmented tracking controller (ATC).

Test A: The performance of the aforementioned control schemes in regulating the v_o , at a step-reference of +10.0 V, is tested under normal conditions. The transistor M is kept turned-on during the experiment. The resulting variations in v_o , exhibited by each of the three controllers, are shown in Fig. 5, 6, and 7, respectively. The analysis of the graphical results clearly validates the superior performance of the ATC. The auxiliary integral state-feedback minimizes the steady-state error and damps the overshoot. The self-tuning DRC significantly improves the transient response as compared to that of LQT and LQIT. The corresponding variations in K_d are shown in Fig. 8.

Test B: The robustness of each controller is tested under load-disturbance conditions. This is done by switching-off the transistor M at $t \approx 1.46$ s. This switching phenomenon leads to an incremental load-step transient. The resulting abrupt variations occurring in the steady-state response are illustrated in Fig. 9, 10, and 11. The ATC effectively rejects the impulsive disturbance, while exhibiting the fastest error convergence rate. The variations in K_d are shown in Fig. 12.

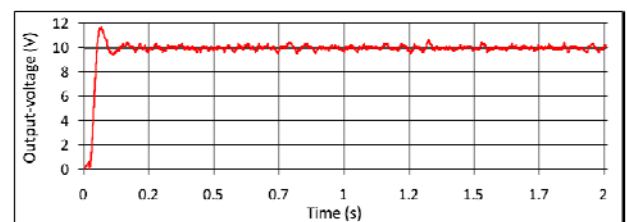


Fig. 5. Step-response of LQT.

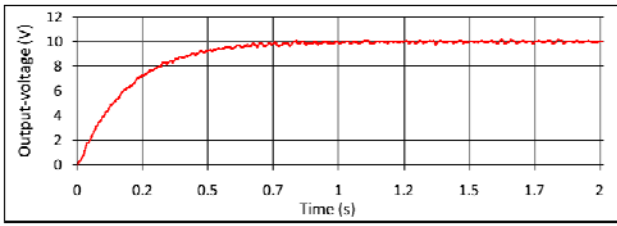


Fig. 6. Step-response of LQIT.

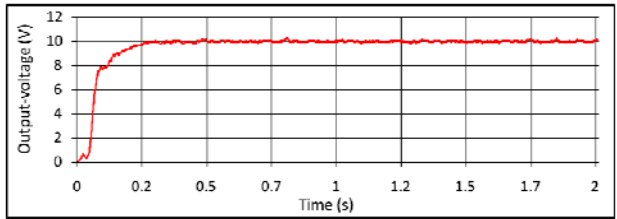


Fig. 7. Step-response of ATC.

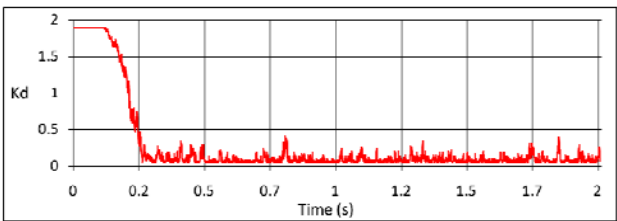


Fig. 8. Variations in K_d under step-reference.

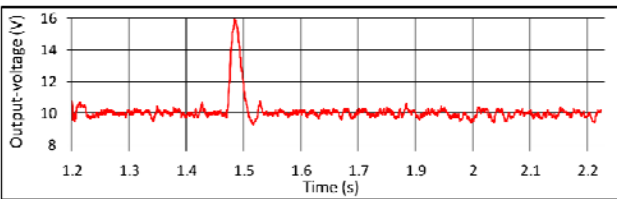


Fig. 9. Response of LQIT under load-step disturbance.

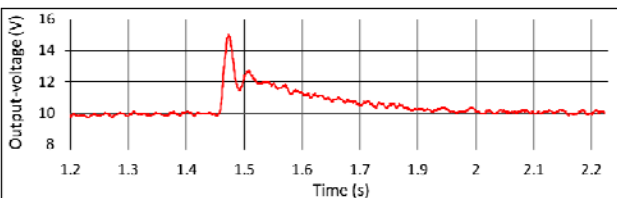


Fig. 10. Response of LQIT under load-step disturbance.

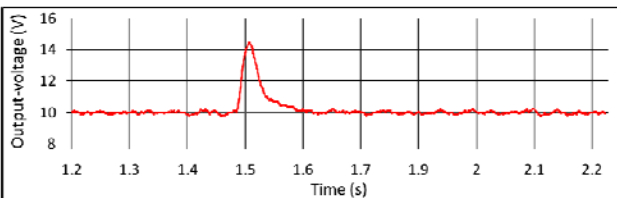


Fig. 11. Response of ATC under load-step disturbance.

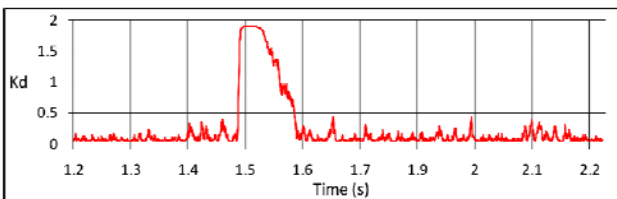


Fig. 12. Variations in K_d under load-step disturbance

Test C: The robustness of each controller is tested by abruptly decreasing the input voltage from 30.0 V to 25.0 V. The corresponding perturbations exhibited by the response of v_o are illustrated in Fig. 13, 14, and 15, respectively. The conventional LQT controller response demonstrates decaying oscillations as it recovers from the disturbance and converges to the steady-state. The LQIT controller effectively damps the oscillations. However, it converges very slowly to the reference-voltage level. The ATC effectively damps the oscillations caused by the fluctuations in v_{in} and quickly converges to reference-voltage level. The corresponding variations in K_d are shown in Fig. 16.

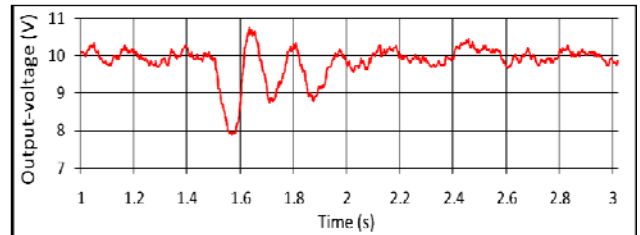


Fig. 13. Response of LQT under input-voltage disturbance.

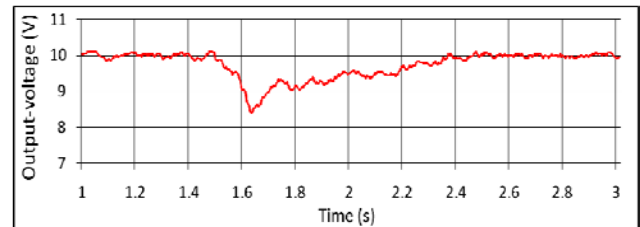


Fig. 14. Response of LQIT under input-voltage disturbance.

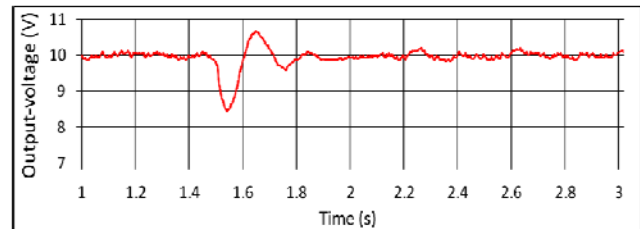


Fig. 15. Response of ATC under input-voltage disturbance.

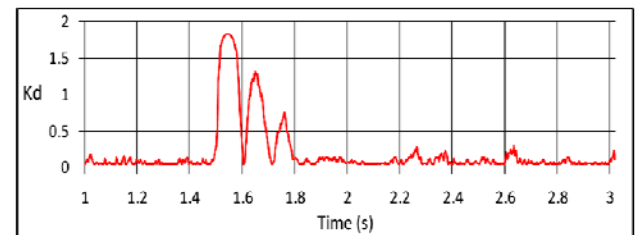


Fig. 16. Variations in K_d under input-voltage disturbance.

Test D: The trajectory tracking performance of each controller is tested by applying a square-wave reference input signal. The reference signal oscillates between discrete voltage-levels of +16.0 V and +4.0 V, after a regular interval of 1.25 s. The corresponding response of v_o , under the influence of each controller, is illustrated in Fig. 17, 18, and 19, respectively. The ATC tracks the abrupt variations in v_{ref} with a significantly improved transient and steady-state response. The variations in K_d are shown in Fig. 20.

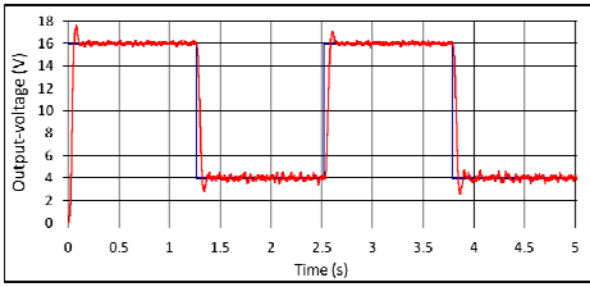


Fig. 17. Square-wave tracking response of LQT.

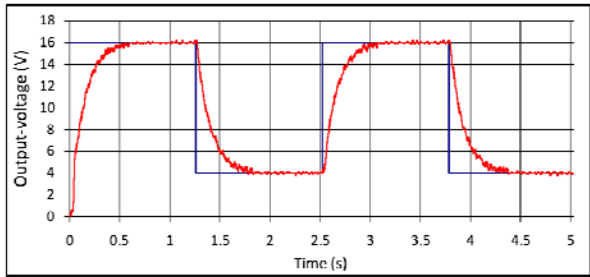


Fig. 18. Square-wave tracking response of LQIT.

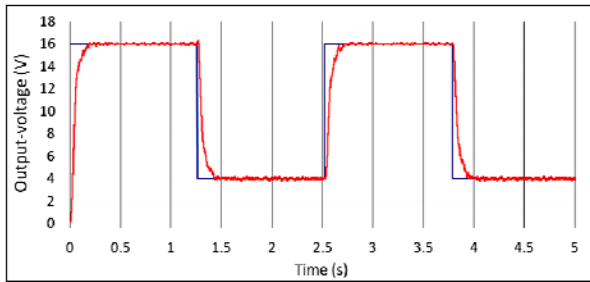


Fig. 19. Square-wave tracking response of ATC.

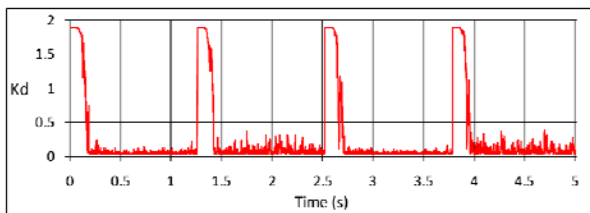


Fig. 20. Variations in K_d under square-wave tracking.

Test E: The trajectory tracking performance of each controller is tested by applying a triangular-wave reference input signal. The reference signal oscillates between +16.0 V and +4.0V in the form of a ramp. The oscillation frequency of the reference signal is set to 0.4 Hz. The corresponding perturbations occurring in the response of v_o , under the influence of each of the three controllers, are illustrated in Figure 21, 22, and 23, respectively. The graphical responses validate the superiority of the trajectory tracking performance exhibited by ATC over the LQT and LQIT. The LQT's response exhibits significant tracking error. The response of LQIT consistently lags behind the reference trajectory by 0.1s while tracking it. The ATC's response accurately tracks the trajectory with negligible lag and minimal tracking error. The corresponding variations in K_d are shown in Fig. 24.

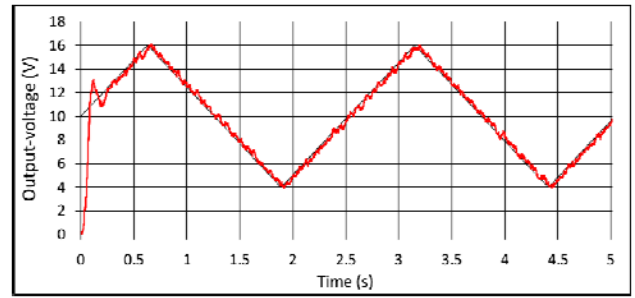


Fig. 21. Triangular-wave tracking response of LQT.

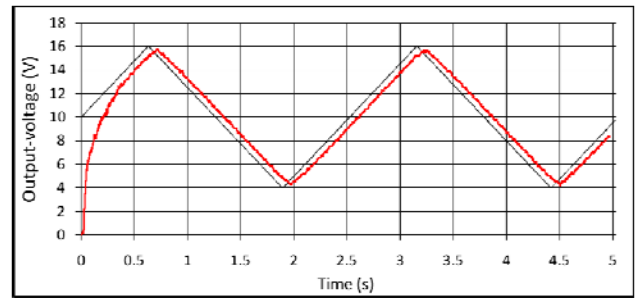


Fig. 22. Triangular-wave tracking response of LQIT.

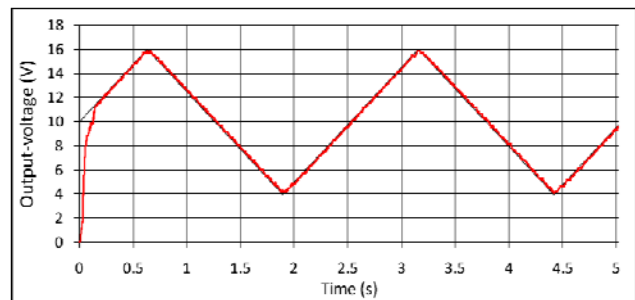


Fig. 23. Triangular-wave tracking response of ATC.

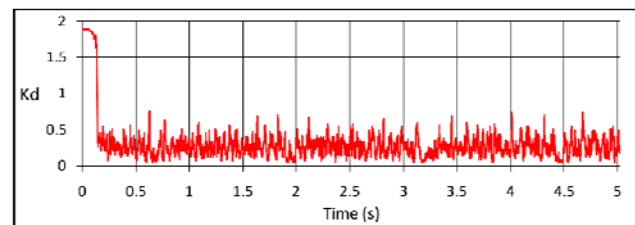


Fig. 24. Variations in K_d under triangular-wave tracking.

The comparative performance assessment of the test results is summarized in Table 2. The responses rendered by each controller, for each test, are analyzed in terms of the rise-time (t_r), over-shoot or undershoot (M_p), settling-time (t_s), and root-mean-square of the steady-state error (e_{ss}).

6. CONCLUSION

This paper presents an augmented affine state-feedback control scheme to robustify the output-voltage regulation and tracking control of a low power DC-DC buck converter. Apart from improving the trajectory tracking performance, the ATC significantly enhances the system's robustness against bounded exogenous disturbances. It also improves the

error convergence-rate of the system and effectively minimizes its steady-state error. The proposed controller achieves the desired performance objectives by augmenting a conventional LQT with auxiliary control components.

Table 2. Summary of test results.

Test	Controller	t_r (s)	M_p (%)	t_s (s)	e_{ss} (V)
A	LQT	0.09	17.45	0.13	0.85
	LQIT	0.49	0.01	0.71	0.13
	ATC	0.18	0.06	0.20	0.16
B	LQT	-	60.0	0.06	-
	LQIT	-	49.8	0.44	-
	ATC	-	44.3	0.11	-
C	LQT	-	21.1	0.49	-
	LQIT	-	15.2	0.83	-
	ATC	-	13.6	0.31	-
D	LQT	0.11	12.42	0.18	0.88
	LQIT	0.50	0.01	0.68	0.18
	ATC	0.20	0.04	0.23	0.17
E	LQT	0.09	15.56	0.29	0.79
	LQIT	0.49	0.01	-	1.12
	ATC	0.18	0.04	0.20	0.16

The summary of experimental results completely validates the efficacy rendered by the proposed augmentations in the control mechanism. The ATC controller exhibits relatively faster transient recovery while effectively suppressing the fluctuations and oscillations upon convergence. Despite the evident performance-improvement and time-optimality yielded by the proposed controller, there is still a lot of room for future enhancements. Firstly, the LQT can be replaced by other model-based controllers; such as, model-predictive-controllers and linear-quadratic-gaussian-trackers etc. Secondly, computationally intelligent adaptation algorithms can also be investigated for the self-tuning of K_d . Thirdly, different meta-heuristic or gradient-based optimization techniques can be investigated to optimally select the Q and R weighting matrices of the LQ cost function. Finally, the proposed controller's robustness can be further examined by using it to control the v_o response of other power electronic converters; such as, Cuk, Sepic, or Zeta converter, etc.

REFERENCES

Akter, P., Uddin, M., Mekhilef, S., Tan, N.M.L., and Akagi, H. (2015). Model predictive control of bidirectional isolated DC-DC converter for energy conversion system.

- International Journal of Electronics*, 102(8), pp. 1407-1427.
- Anbarasi, S., and Muralidharan, S. (2016). Enhancing the Transient Performances and Stability of AVR System with BFOA Tuned PID Controller. *Control Engineering and Applied Informatics*, 18(1), pp. 20-29.
- Antão, R., Mota, A., and Martins, R.E. (2014). Adaptive control of a buck converter with an ARM Cortex-M4. In: *Proceedings of 2014 16th International Power Electronics and Motion Control Conference and Exposition*, Antalya, Turkey, pp. 359-364.
- Aryani, D.R., Kim, J.S., and Song, H. (2017). Interlink Converter with Linear Quadratic Regulator Based Current Control for Hybrid AC/DC Microgrid. *Energies*, 10(11), pp. 1-26.
- Babazadeh, A., and Maksimovic, D. (2009). Hybrid Digital Adaptive Control for Fast Transient Response in Synchronous Buck DC-DC Converters. *IEEE Transactions on Power Electronics*, 24(1), pp. 2625-2638.
- Bagewadi, M.D., and Dambhare, S.S. (2017). A novel hybrid converter derived from buck-boost circuit for standalone applications. In: *Proceedings of 2017 19th European Conference on Power Electronics and Applications*, Warsaw, Poland, pp. 1-8.
- Benzaouia, A., Soliman, H.M., and Saleem, A. (2016). Regional pole placement with saturated control for DC-DC buck converter through Hardware-in-the-Loop. *Transactions of the Institute of Measurement and Control*, 38(9), pp. 1041-1052
- Bhaumik, A., Kumar, Y., Srivastava, S., and Islam, S.M. (2016). Performance studies of a separately excited DC motor speed control fed by a buck converter using optimized PI λ D μ controller. In: *Proceedings of 2016 International Conference on Circuit, Power and Computing Technologies*, Nagercoil, India, pp. 1-6.
- Boutouba, M., El-Ougli, A., Miqui, S., and Tidhaf, B. (2017). Intelligent control for voltage regulation system via DC-DC Converter using Raspberry Pi 2 board. *WSEAS Transactions on Electronics*, 8, pp. 41-47.
- Corradini, L., Babazadeh, A., Bjeletic, A., and Maksimovic, D. (2010). Current-Limited Time-Optimal Response in Digitally Controlled DC-DC Converters. *IEEE Transactions on Power Electronics*, 25(11), pp. 2869 – 2880.
- Cui, H., Yang, J., and Li, S. (2014). Nonlinear disturbance rejection control for a buck-boost converter with load uncertainties. In: *Proceedings of 2014 33rd Chinese Control Conference*, Nanjing, China, pp. 3788-3793.
- Dobra, P., Trusca, M., Moga, D., and Petreus, D. (2007). Stability aspects in DC-DC converters using PID controller. *Control Engineering and Applied Informatics*, 9(1), pp. 33-40.
- Duong, M.Q., Nguyen, V.T., Sava, G.N., Scripcariu, M., and Mussetta, M. (2017). Design and simulation of PI-type control for the Buck Boost converter. In: *Proceedings of 2017 International Conference on Energy and Environment*, Bucharest, Romania, pp. 79-82.
- Dupont, F.H., Montagner, V.F., Pinheiro, J.R., Pinheiro, H., Oliveira, S.V.G., and Péres, A. (2013). Comparison of

- Linear Quadratic Controllers with stability analysis for DC-DC boost converters under large load range. *Advances in Fractional Order Control and Estimation*, 15(3), pp. 861-871.
- Ghartemani, M.K., Khajehoddin, S.A., Praveen Jain, P., and Bakhshai, A. (2011). Linear quadratic output tracking and disturbance rejection. *International Journal of Control*, 84(8), pp. 1442-1449.
- Ghosh, A., and Banerjee, S. (2015). Control of Switched-Mode Boost Converter by using classical and optimized Type controllers. *Control Engineering and Applied Informatics*, 17(4), pp. 114-125.
- Guo, B., Hu, L., and Bai, Y. (2012). A nonlinear PID controller with tracking differentiator applying in BLDCM servo system. In: *Proceedings of 2012 7th International Power Electronics and Motion Control Conference*, Harbin, China, pp. 2467-2471.
- Guo, L., Hung, J.Y., and Nelms, R.M. (2009). Evaluation of DSP-Based PID and Fuzzy Controllers for DC-DC Converters. *IEEE Transactions on Industrial Electronics*, 56(6), pp. 2237 – 2248.
- He, G.Z., Juang, Y.T, Tsai, J.S.H., Lin, Y.Y., Guo, S.M., Shieh, L.S., and Tsai, T.J. (2017). An effective optimal linear quadratic analog tracker for the system with unknown disturbances. In: *Proceedings of 2017 IEEE 26th International Symposium on Industrial Electronics*, Edinburgh, UK, pp. 412-417.
- Hossain, M.Z., Rahim, N.A., and Selvaraj, J. (2018). Recent progress and development on power DC-DC converter topology, control, design and applications: A review. *Renewable and Sustainable Energy Reviews*, 81(1), pp. 205-230.
- Isayed, B.M., and Hawwa, M.A. (2007). A nonlinear PID control scheme for hard disk drive servosystems. In: *Proceedings of 2007 15th Mediterranean Conference on Control & Automation*, Athens, Greece, pp. 1-6.
- Jaen, C., Pou, J., Pindado, R., Sala, V., and Zaragoza, J. (2006). A Linear-Quadratic Regulator with Integral Action Applied to PWM DC-DC Converters. In: *Proceedings of 32nd IEEE Annual Conference on Industrial Electronics*, Paris, France, pp. 2280 – 2285.
- Jalilvand, A., Vahedi, H., and Bayat, A. (2010). Optimal Tuning of the PID Controller for a Buck Converter Using Bacterial Foraging Algorithm. *Proceedings of IEEE International Conference on Intelligent and Advanced Systems*, Kuala Lumpur, Malaysia, pp. 1-5.
- Kapat, S., and Krein, P.T. (2012). Improved Time Optimal Control of a Buck Converter Based on Capacitor Current. *IEEE Transactions on Power Electronics*. 27(3), pp. 1444-1454.
- Kapat, S., and Krein, P.T. (2012). Formulation of PID Control for DC-DC Converters based on Capacitor Current: A Geometric Context. *IEEE Transactions on Power Electronics*, 27(3), pp. 1424-1432.
- Karanjkar, D.S., Chatterji, S., and Kumar, A. (2014). Development of linear quadratic regulator based PI controller for maximum power point tracking in solar photo-voltaic system. In: *Proceedings of 2014 Recent Advances in Engineering and Computational Sciences*, Chandigarh, India, pp. 1-6.
- Kiumarsi, B., Lewis, F.L., Naghibi-Sistani, M.B., and Karimpour, A. (2015). Optimal Tracking Control of Unknown Discrete-Time Linear Systems Using Input-Output Measured Data. *IEEE Transactions on Cybernetics*, 45(12), pp. 2770 – 2779.
- Kumar, A., Vempati, A.S., and Behera, L. (2013). T-S fuzzy model based Maximum Power Point Tracking control of photovoltaic system. In: *Proceedings of 2013 IEEE International Conference on Fuzzy Systems*, Hyderabad, India, pp. 1-8.
- Lakshmi, S., and Raja, T.S.R. (2014). Design and implementation of an observer controller for a buck converter. *Turkish Journal of Electrical Engineering and Computer Sciences*, 22(3), pp. 562-572.
- Lambert, W.J., Ayyanar, R., and Chickamenahalli, S. (2009). Fast Load Transient Regulation of Low-Voltage Converters with the Low-Voltage Transient Processor. *IEEE Transactions on Power Electronics*, 24(7), pp. 1839-1854.
- Lee, B.S., Kim, S.K., Park, J.H., and Lee, K.B. (2016). Adaptive output voltage tracking controller for uncertain DC/DC boost converter. *International Journal of Electronics*, 103(6), pp. 1002-1017.
- Lewis, F.L., Vrabie, D., and Syrmos, V.L. (2012). *Optimal Control*. John Wiley and Sons, New Jersey, USA.
- Lian, K.Y., Liu, C.H., and Chiu, C.S. (2017). Robust Fuzzy Output Regulator Design for Nonlinear Systems without Virtual Desired Variable Calculation. *Control Engineering and Applied Informatics*, 19(1), pp. 27-36.
- Lindiya, A., Palani, S., and Iyyappan. (2012). Performance comparison of various controllers for DC-DC Synchronous Buck Converter. *Procedia Engineering*, 38, pp. 2679-2693.
- Lindiya, S.A., Vijayarekha. K., and Palani, S. (2016). Deterministic LQR Controller for DC-DC Buck Converter. In: *Proceedings of IEEE Biennial International Conference on Power and Energy Systems*, Bangalore, India, pp. 1-6.
- Maccari, L.A., Montagner, V.F., and Ferreira, A.A. (2013). A linear quadratic control applied to buck converters with H-infinity constraints. In: *Proceedings of 2013 IEEE Brazilian Power Electronics Conference*, Gramado, Brazil, pp. 339-344.
- Mariethoz, S., Almer, S., Baja, M., Beccuti, A.G., Patino, D., Wernrud, A., Buisson, J., Cormerais, H., Geyer, T., Fujioka, H., Jonsson, U.T., Kao, C.Y., Morari, M., Papafotiou, G., Rantzer, A., and Riedinger, P. (2010). Comparison of Hybrid Control Techniques for Buck and Boost DC-DC Converters. *IEEE Transactions on Control Systems Technology*, 18(5), pp. 1126-1145.
- Mahendran, V., and Ramabadrhan, R. (2016). Fuzzy-PI-based centralised control of semi-isolated FP-SEPIC/ZETA BDC in a PV/battery hybrid system. *International Journal of Electronics*, 103(11), pp. 1909-1927.
- McIntyre, M.L., Mohebbi, M., and Latham, J. (2015). Nonlinear current observer for backstepping control of buck-type converters. In: *Proceedings of 2015 IEEE 16th Workshop on Control and Modeling for Power Electronics*, Vancouver, BC, Canada, pp. 1-7.

- Modares, H., and Lewis, F.L. (2014). Linear Quadratic Tracking Control of Partially-Unknown Continuous-Time Systems Using Reinforcement Learning. *IEEE Transactions on Automatic Control*, 59(11), pp. 3051-3056
- Mohan, N., Undeland, T.M., and Robbins, W.P. (2007). *Power electronics: converters, applications, and design*, Wiley, New Delhi, India.
- Moreira, C.O., Silva, F.A., Pinto, S.F., and Santos, M.B. (2011). Digital LQR control with Kalman Estimator for DC-DC Buck converter. In: *Proceedings of IEEE International Conference on Computer as a Tool*, Lisbon, Portugal, pp. 1-4.
- Naik, M.G., LovaLakshmi, T., and Harinarayana. T. (2015). Modeling and Design of Robust LQI Controller for DC-DC Buck Converter. *International Journal and Magazine of Engineering, Technology, Management and Research*, 2(12), pp. 818-823.
- Olalla, C., Queinnec, I., Leyva, R., and El-Aroudi, A. (2011). Robust optimal control of bilinear DC-DC converters. *Control Engineering Practice*, 19(7), pp. 688-699.
- Pedroso, M.D., Nascimento, C.B., Tuset, A.M., and Kaster, M. S. (2013). Performance comparison between nonlinear and linear controllers applied to a buck converter using poles placement design. In: *Proceedings of 15th IEEE European Conference on Power Electronics and Applications*, Lille, France, pp. 1-10.
- Pedroso, M.D., Nascimento, C.B., Tuset, A.M., and Kaster, M.S. (2013). A Hyperbolic Tangent Adaptive PID + LQR Control Applied to a Step-Down Converter Using Poles Placement Design Implemented in FPGA. *Mathematical Problems in Engineering*, 2013, pp. 1-8.
- Peretz, M.M., and Yaakov, S.B. (2012). Time-Domain Design of Digital Compensators for PWM DC-DC Converters," *IEEE Transactions on Power Electronics*, 27(1), pp. 284 - 293.
- Pitel, G.E., and Krein, P.T (2009). Minimum-Time Transient Recovery for DC-DC Converters Using Raster Control Surfaces. *IEEE Transactions on Power Electronics*, 24(12), pp. 2692 – 2703.
- Priewasser, R., Agostinelli, M., Unterrieder, C., Marsili, S., and Huemer, M. (2014). Modeling, Control, and Implementation of DC-DC Converters for Variable Frequency Operation. *IEEE Transactions on Power Electronics*, 29(1), pp. 287-301.
- Qi, W., Li, S., Tan, S.C., and Hui, S.Y.R. (2018). Parabolic-Modulated Sliding-Mode Voltage Control of a Buck Converter. *IEEE Transactions on Industrial Electronics*, 65(1), pp. 844 – 854.
- Reis, F.E.U., Bascopé, R.P.T., and Costa, M.V.S. (2011). LQR control with integral action applied to a high gain step-up DC-DC converter. In: *Proceedings of 2011 Brazilian Power Electronics Conference*, PraiaMar, Brazil, pp. 256-261.
- Ruderman, M., Krettek, J., Hoffmann, F., and Bertram, T. (2008). Optimal State Space Control of DC Motor. In: *Proceedings of the 17th World Congress. The International Federation of Automatic Control*, Seoul, Korea, pp. 5796-5801.
- Saleem, O., Hassan, H., Khan, A., and Javaid, U. (2017). Adaptive Fuzzy-PD Tracking Controller for Optimal Visual-Servoing of Wheeled Mobile Robots. *Control Engineering and Applied Informatics*, 19(3), pp. 56-68.
- Saleem, O., and Omer, U. (2017). EKF-based self-regulation of an adaptive nonlinear PI speed controller for a DC motor. *Turkish Journal of Electrical Engineering and Computer Sciences*, 25(5), pp. 4131 – 4141.
- Saleem, O., and Omer, U. (2017). Synergistic speed control strategy for PMDC motor. In: *Proceedings of 2017 IEEE International Multi-topic Conference*, Lahore, Pakistan, pp. 1-6.
- Seraji, H. (1998). A new class of non-linear PID controller with robotic applications. *Journal of Robotic Systems*, 15, pp. 161-181.
- Seshagiri, S., Block, E., Larrea, I., and Soares, L. (2016). Optimal PID Design for Voltage Mode Control of DC-DC Buck Converters. In: *Proceedings of IEEE Indian Control Conference*, Hyderabad, India, pp. 99-104.
- Spinu, V., Lisi, S., and Lazar, M. (2014). Constrained reference tracking for a high-speed buck converter. In: *Proceedings of 2014 IEEE Conference on Control Applications*, Juan Les Antibes, France, pp. 1255-1260.
- Tahri, F., Tahri, A., Allali, A., and Flazi, S. (2012). The Digital Self-Tuning Control of a Step Down DC-DC Converter. *Acta Polytechnica Hungarica*, 9(6), pp. 49-64.
- Tan, G.Q., Chen, Y.H., and Gu, L. (2014). LQR Based Optimal PID Control for Buck Converter. *Applied Mechanics and Materials*, 687-691, pp. 3221-3226.
- Zhu, D., Liu, L., and Liu, C. (2014). Optimal fractional-order PID control of chaos in the fractional-order BUCK converter. In: *Proceedings of 2014 IEEE 9th Conference on Industrial Electronics and Applications*, Hangzhou, China, pp. 787-791.